Statistical Assessment of CHAMP Data and Models Using the Energy Balance Approach

Jürgen Kusche and Jasper van Loon

TU Delft/DEOS, 2600 GB Delft, P.O. Box 5058, The Netherlands
j.kusche@lr.tudelft.nl, *j.p.vanloon@lr.tudelft.nl*

Summary. The energy balance approach is used for a statistical assessment of CHAMP orbits, data and gravity models. It is known that the quality of GPS–derived orbits varies and that CHAMP accelerometer errors are difficult to model. This makes the selection of orbits for gravity recovery difficult. Here we identify the noise level present in in–situ potential values from the energy balance in an iterative variance–component estimation. This means we solve simultaneously for a spherical harmonic model, for polynomial coefficients absorbing accelerometer drift, and for sub–daily noise variance components. These should be understood in a sense of model consistency. Using dynamic GFZ orbits, results including 92 days in 2002 indicate that for most days the noise is at 0.25–0.3m^2/s^2, with notable exceptions. The corresponding gravity model is found close to EIGEN–2, after two iterations. With TUM kinematic orbits and Lagrange–interpolated velocities or TUM reduced-dynamic orbits, we found for preselected data the consistency at the 0.7-0.8m^2/s^2 (KIN), 0.3-0.35m^2/s^2 (RD) level; gravity models improve significantly on EGM96. Generally, iterative re–weighting improves the solutions significantly, and 'trackiness' is considerably reduced.

Key words: CHAMP, energy balance approach, statistical assessment, variance components

1 Energy Conservation Method

Various groups have demonstrated that the energy balance approach can be used to compute a gravity model from CHAMP reduced-dynamic or kinematic orbits, see Gerlach et al. (2003a,b) or Howe et al. (2003). The approach can also be used to verify the consistency of CHAMP accelerometer data, orbits, gravity field model and other (e.g. tidal) models, and to assess the magnitude of systematic and stochastic errors. We have analyzed CHAMP data for the in–situ potential following Jekeli's method. We have estimated simultaneously corrections to the spherical harmonic coefficients, sub–daily polynomial coefficients describing residual (after applying bias and scale factors from the ACC files) drift of the accelerometer, and sub–daily variance components of the in–situ potential values. A known obstacle for this type of analysis is the selection of 'good' orbits. In our approach, arcs showing spurious behaviour are effectively downweighted within an iterative maximum–likelihood estimation process, which improves our gravity field solution significantly. In turn, the estimation of the individual variance components is improved. As a by–product, we have investigated the correlations of estimated accelerometer drift parameters with the spherical harmonic coefficients.

The theory of the energy balance approach and its potential application to LEO satellite experiments goes back to the 60's, and has been considerably revived re-

cently, see Jekeli (1999), Visser et al. (2003) Ilk and Löcher (in press). We use the following formulation, which is based on expressing all quantities of interest in an inertial coordinate system:

$$T(t) - V^{\mathrm{ref}}(t) - \delta V(t) - R(t) = E_0 + \int_{t_0}^{t} \boldsymbol{f} \cdot \dot{\boldsymbol{x}}\, d\tau + \int_{t_0}^{t} \boldsymbol{\nabla} V^{\mathrm{tides}} \cdot \dot{\boldsymbol{x}}\, d\tau \quad (1)$$

Here $T = \frac{1}{2}|\dot{\boldsymbol{x}}|^2$ is the kinetic potential, V^{ref} is a static reference potential appearing time–dependent in inertial coordinates, δV is a residual geopotential that we parameterize by spherical harmonics whose coefficients $\delta c_{lm}, \delta s_{lm}$ are to be solved for, R is the potential rotation term which approximates the potential contribution $\int_{t_0}^{t} \frac{\partial V}{\partial t}\, d\tau \approx -\omega_e(x_1\dot{x}_2 - x_2\dot{x}_1)$ (up to a constant, see Jekeli 1999) of the rotating earth in inertial space, and E_0 is a constant. Furthermore, $\boldsymbol{f}$ are corrected measurements from CHAMP's STAR accelerometer to account for non–conservative forces, and the last term on the right–hand side accommodates for tidal effects by evaluating the corresponding work integral. We found that neglecting the explicit time–variation of the tidal potentials by simply evaluating $V^{\mathrm{tides}}(t)$ would be possible but introduces low–frequency drift effects that propagate into the low–order correction polynomial coefficients (see below). We model the direct attraction by sun and moon from JPL DE ephemeris, the solid earth tides following the IERS conventions, plus ocean tides (GOT 99.2).

2 Statistical Assessment and Estimation Procedure

The energy balance approach uses eq (1) for combining orbit, accelerometry data, reference geopotential model, tidal corrections and auxiliary information (e.g. earth rotation) into a preprocessed stream of pseudo–observations, $\delta V(t)$, which can be used without further linearization to estimate the $\delta c_{lm}, \delta s_{lm}$. Consequently, position errors $\boldsymbol{\epsilon_x}$, velocity errors $\boldsymbol{\epsilon_{\dot{x}}}$, accelerometry errors $\boldsymbol{\epsilon_f}$ and tide model errors affect the in–situ potential differences (see Visser et al., 2003) approximately as

$$\epsilon_V = \dot{\boldsymbol{x}} \cdot \boldsymbol{\epsilon_{\dot{x}}} - \nabla V^{\mathrm{ref}} \cdot \boldsymbol{\epsilon_x} - \omega_e(\epsilon_{x_1}\dot{x}_2 - \epsilon_{x_2}\dot{x}_1) - \omega_e(x_1\epsilon_{\dot{x}_2} - x_2\epsilon_{\dot{x}_1}) + \int_{t_0}^{t} \boldsymbol{\epsilon_f} \cdot \dot{\boldsymbol{x}}\, d\tau + \delta V^{\mathrm{tides}} \quad (2)$$

It is clear that accelerometer biases and scaling errors, predominantly in the in–flight axis, cause in first approximation a linear drift in the δV measurement. It is also known that if an erroneous reference model went into the computation of (reduced–) dynamic orbits, resulting orbit errors will compensate to a certain extend for this in the energy balance (1), and an estimated gravity model will be biased. This is why we use the term noise variance in a sense of consistency. Knowing the variance of the potential difference error, $\sigma^2(\delta V) = E\{\epsilon_V^2\}$, we can set up a weighted least square adjustment which would suppress spurious arcs by downweighting. This noise variance, however, is nonstationary and difficult to assess a priori. The orbits, on the other hand, are given in batches of 0.5–1.5 day length dependent on the POD analysis strategy. Here we assign an unknown variance component $\sigma_k^2(\delta V)$ to

each batch and estimate it jointly with the residual gravity field and with parameters that account for accelerometer drift. Written as a Gauss–Markov model, this is

$$\boldsymbol{A}_k \begin{pmatrix} \boldsymbol{x}_{\mathrm{SH}} \\ \boldsymbol{x}_{\mathrm{ACC}_1} \\ \cdots \\ \boldsymbol{x}_{\mathrm{ACC}_p} \end{pmatrix} - \boldsymbol{y}_k = \boldsymbol{\epsilon}_k \qquad \begin{matrix} D(\boldsymbol{\epsilon}_k) = \sigma^2_{(k)} \boldsymbol{I} \\ D(\boldsymbol{x}_{\mathrm{SH}}) = \sigma^2_{(0)} \boldsymbol{R} \end{matrix} \qquad k = 1 \ldots p \qquad (3)$$

where $\boldsymbol{x}_{\mathrm{SH}}$ contains SH coefficients, $\boldsymbol{x}_{\mathrm{ACC}_k}$ and $\sigma^2_{(k)}$ are drift parameters and variance components for the k–th data set, and $\sigma^2_{(0)}$ is a regularization parameter if needed. This requires an iterative strategy involving re–weightings of the contributions, synthesis of potential residuals, and repeated solutions of the overall LS problem. A fast Monte Carlo machinery for implementing maximum–likelihood estimation has been developed in Koch and Kusche (2002) and tested in Kusche (2003) on a simulated LEO gravity recovery problem. Weighting factors for combination solutions can be computed the same way. At convergence the results of ML estimation equal those of the iterated MINQUE technique. It should be emphasized that from the point of view of estimating drift parameters for each batch k of data, it would be preferable to have short batches comprising an orbital revolution each. From the statistical analysis point, we must keep the number of solved–for variance components limited to maintain fast convergence of our algorithm.

3 Analysis of GFZ dynamic orbits

We used 92 days of GFZ's PSO and ACC data, of the first half 2002 and without preselection. These are broken up into daily/half–daily batches. We solve for a SH expansion to degree 75, for 4 polynomial parameters per day to account for accelerometer drift in the form $\epsilon(t) = \sum_{n=0}^{3} a_n^k (t - t_k)^n$, and for a daily variance σ_k^2. Arc–dependent a_n^k parameters are eliminated from the normal system by the method of partitioning and backsubstitution. The gravity field model that went into GFZ's dynamic PSO orbits is not completely identical to EIGEN–2 (P. Schwintzer, pers. comm.), and we treat it as unknown here. In the first iteration, all batches are weighted equally. Fig. 1 shows the estimated σ_k's after the second iteration where practically convergence is reached. Fig. 3 (left) shows the difference of the residual gravity field with respect to GFZ's published EIGEN–2 solution (Reigber et al., 2003) without re–weightings (0th iteration), in geoid heights. Fig. 3 (right) shows the difference, complete to degree 70, after arriving at convergence. No data has been removed, but all spurious orbits are downweighted. It should be noted that for EIGEN–2 data from a different time period was used than we used in this study.

4 TUM kinematic and reduced–dynamic orbits

We have further investigated about 100 days of kinematic CHAMP orbits, which were kindly provided by D. Svehla by IAPG, TU Munich. These orbits are processed following the zero–differencing strategy, see Svehla and Rothacher (2003), and were provided with full variance–covariance information per data point. In

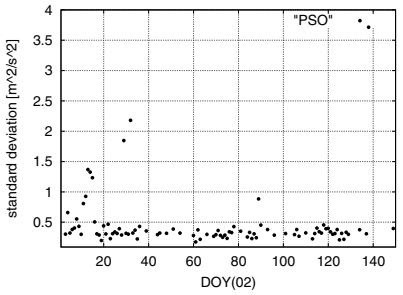

Fig. 1. $\sigma_k^2(\delta V)$ for DOY 002–148 (2002), PSO orbits

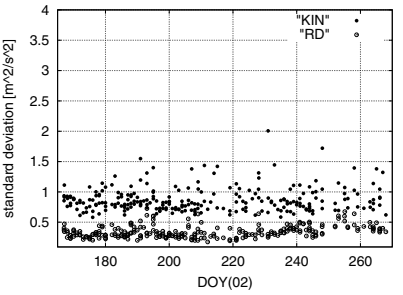

Fig. 2. $\sigma_k^2(\delta V)$ for DOY 167–268 (2002), KIN and RD orbits

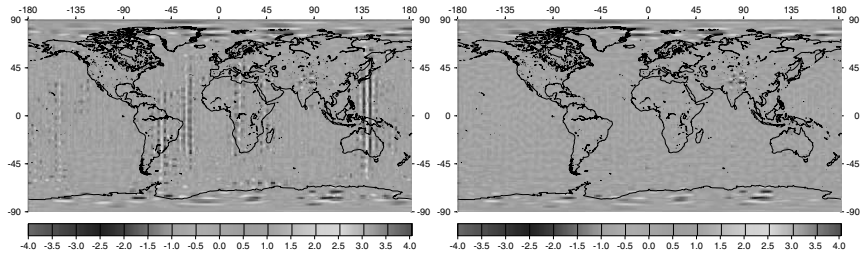

Fig. 3. Difference to EIGEN–2 [m]. Left: L=75, 0th iteration. Right: L=70, after 2nd iteration

a preprocessing step we have removed all kinematic positions to which a–priori sigma's of larger than 5cm in either x, y, or z were assigned. Furthermore, only data segments of at least 2.5h have been selected. To allow a clean comparison afterwards, we have based our selection on purpose not on comparing KIN and RD orbits. After this, the used data corresponds to about 52 days. Kinematic orbit determination does not provide velocities, so we had to compute CHAMP velocities using a Lagrange 7–point interpolator. We avoid any smoothing at this step. In what follows, the same analysis has been performed as with the GFZ PSO data. One must, however, bear in mind that KIN orbits are completely independent from any prior gravity field, that they are spaced at 30s intervals, and that the interpolator used for deriving velocities is of influence. In addition, we have taken TUM RD orbits for the same time periods and repeated the procedure (apart from the Lagrange interpolation). Results for the noise levels are shown in Fig. 2.

In summary, one can state that the estimated variance components for the KIN orbits are roughly at the 0.7–0.8m^2/s^2 level, whereas those for the RD orbits are at the 0.3–0.35m^2/s^2 level, with exceptions and a slight increase at about DOY 250. According to eq. (2), assuming that the velocity error dominates, this indicates that velocities from Lagrange interpolation have an accuracy of about 1mm/s. We have compared these directly with RD velocities and found this error level confirmed. Note that we have based our orbit selection on purpose not on a–priori comparison of KIN and RD orbits; which would have given a more optimistic error level. Fig. 4 shows for the estimated gravity field solutions the signal de-

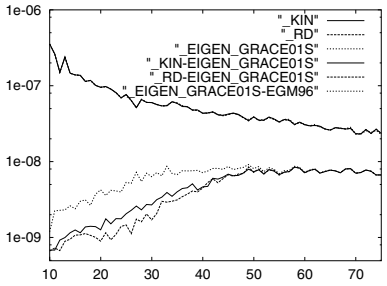

Fig. 4. Degree variances. Solutions with TUM KIN, RD orbits

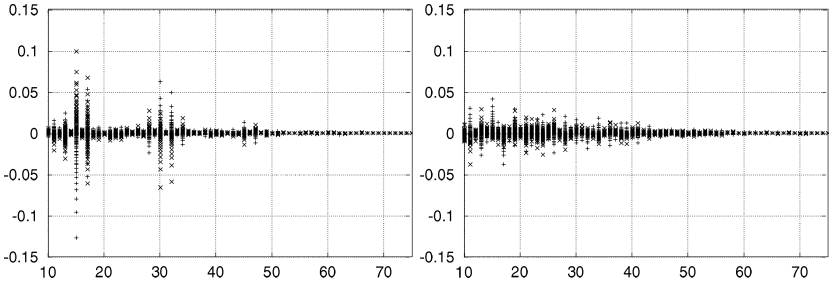

Fig. 5. Correlation of a_0 (+) and a_1 (×) with the $\delta c_{lm}, \delta s_{lm}$. Left: arc length 16h. Right: 3h.

gree variances and the difference degree variance with respect to the recently published EIGEN–GRACE01S model (Reigber et al, in preparation). For comparison, EGM96 (Lemoine et al., 1998) is also shown, which has been used as a reference field in the computation. Both KIN and RD solution show clear improvements towards the EIGEN–GRACE01S, when compared with the EGM96 model. Due to regularization, there is almost no signal left beyond degree 50 and the reference solution EGM96 dominates. It is obvious that between degrees 15 and 40 the reduced-dynamic solution is somewhat closer to the GRACE model; probably because CHAMP data are already enclosed in the prior gravity model used for computing the RD orbits. We believe that the timespan we used is too short to draw further conclusions.

In our treatment the determination of arc–dependent accelerometer drift parameters a_n^k is part of the estimation procedure and not a separate preprocessing step. It is therefore possible to study the correlation between the a_n^k and the SH coefficients from the a–posteriori covariance matrix. In Fig. 5 we show as an example correlation coefficients of the estimated energy constant $a_0 \equiv E_0$ (+) and of the slope parameter a_1 (×) with the $\delta c_{lm}, \delta s_{lm}$ per degree, for arc lengths of 16 hours and 3 hours. The correlation between estimates for a_0 and a_1 is much higher and increases for short arc length. However, as indicated in the figures, there appears to be no estimability problem so far. We plan to extend this type of correlation studies, in particular when incorporating longer data sets and time–variable low–degree SH coefficients.

5 Discussion and Outlook

We have discussed a statistical assessment of CHAMP orbits and data within the energy balance method. Non–stationary noise has been modelled with piecewise constant variance. We have proven that we can efficiently estimate individual noise levels for data batches, and that gravity solutions using an optimally weighted LS procedure are superior to heuristic weighting. Our results indicate that the consistency of GFZ PSO orbits is at 0.25–0.3m^2/s^2 for the time interval that we considered, with notable exceptions. TUM orbits were found at levels of 0.7–0.8m^2/s^2 (KIN) and 0.3–0.35m^2/s^2 (RD). This is due to the different POD processing strategies, and these figures should be interpreted with care. We have estimated gravity models which we believe clearly improve on pre–CHAMP models. More orbits have to be added to make final statements on the quality of these models. In particular, velocity derivation from KIN orbits needs to be investigated. Ongoing research includes using more data, and accounting for time–wise correlations. In the meantime, we added CHAMP data from KIN orbits to EGM96 by using its full variance–covariance matrix and determined weighting factors $\sigma_{(0)}$ by ML estimation.

Acknowledgement. We are grateful to GFZ Potsdam for providing CHAMP ACC and PSO data. Thanks go also to IAPG, TU Munich, for providing CHAMP orbits.

References

1. Gerlach C, Sneeuw N, Visser P, Svehla D (2003) CHAMP gravity field recovery with the energy balance approach: first results. in: Reigber et al (Eds): First CHAMP Mission Results for Gravity, Magnetic and Atmospheric Studies, Springer, Berlin: 134–139.
2. Gerlach C and 11 authors (in press). A CHAMP–only gravity field model from kinematic orbits using the energy integral. Submitted to Geophys Res Lett.
3. Howe E, Stenseng L, Tscherning CC (2003) Analysis of one month of state vector and accelerometer data for the recovery of the gravity potential. Adv Geosciences *1*: 1–4.
4. Ilk KH, Löcher A (in press) The use of energy balance relations for validation of gravity field models and orbit determination. presented at IUGG Gen. Ass., 2003, Sapporo.
5. Jekeli C (1999) The determination of gravitational potential differences from satellite–to–satellite tracking. Cel Mech Dyn Astr *75*: 85–100.
6. Koch K–R, Kusche J (2002) Regularization of geopotential determination from satellite data by variance components. J Geodesy *76*: 259–268.
7. Kusche J (2003) A Monte–Carlo technique for weight estimation in satellite geodesy. J Geodesy *76*: 641–652.
8. Lemoine FG and 14 authors (1998) The Development of the Joint NASA GSFC and the National Imagery and Mapping Agency (NIMA) Geopotential Model EGM96, NASA/TP–1998–206861, NASA–GSFC, Greenbelt MD.
9. Reigber C and 12 authors (2003) The CHAMP–only Earth Gravity Model EIGEN–2. Adv Space Res *31(8)*: 1883–1888.
10. Reigber C, Schmidt R, Flechtner F, König R, Meyer U, Neumayer KH, Schwintzer P, Zhu S (in prep.) First EIGEN Gravity Field Model based on GRACE Mission Data Only
11. Svehla D, Rothacher M (2003) Kinematic and reduced–dynamic precise orbit determination of low earth orbiters. Adv Geosciences *1*: 47–56.
12. Visser P, Sneeuw N, Gerlach C (2003) Energy integral method for gravity field determination from satellite orbit coordinates. J Geodesy *77*: 207–216.